182473: migmatitic gneiss, Big Red prospect

(Nornalup Zone, Albany–Fraser Orogen)

Location and sampling

SEEMORE (SH 51-12), CLAYPAN (3837)

MGA Zone 51, 690500E 6649200N

Sampled on 17 August 2010

This sample was collected from diamond drillcore from hole BRDDH001, located on the Big Red prospect, at a depth of 169.2 – 170.2 m. The hole was drilled by Teck Australia Pty Ltd, and was co-funded through the Exploration Incentive Scheme. The drillhole is located on the Nullarbor Plain, approximately 17.0 km south of Fifty Mile Claypan, 38.0 km northeast of Native Willow Bore (Kananda Station), and 55.4 km west of radio mast R204 on the Rawlinna–Warburton Road (Connie Sue Highway).

Tectonic unit/relations

The sample is from drillhole BRDDH001, which intersected Precambrian basement rocks beneath the Mesozoic–Cenozoic Eucla Basin at a depth of 106.4 m; the total depth of the hole was 306.8 m. BRDDH001 was drilled to investigate a magnetic high, interpreted from detailed aeromagnetic data as a potential magnetite-bearing stratigraphic iron-formation, possibly associated with copper–gold mineralization (Tillick, 2010). This anomaly is located within the eastern Nornalup Zone of the Albany–Fraser Orogen, which contains 1800–1760 Ma metagranitic rocks similar in age to some metagranitic rocks in the Biranup Zone, overlain by metasedimentary rocks of the Arid Basin (Spaggiari et al., 2011). The Nornalup Zone is intruded by rocks of the Mesoproterozoic Recherche and Esperance Supersuites (Nelson et al., 1995).

The Precambrian rocks in BRDDH001 comprise interlayered granitic gneiss, metasedimentary gneiss (some of which is strongly magnetic, and possibly represents metamorphosed banded iron-formation), and amphibolite (see also Tillick, 2010). The present sample, GSWA 182473, is from layered, migmatitic gneiss with millimetre- to centimetre-scale, foliation-parallel, dark, biotite-rich layers alternating with pink, K-feldspar- and quartz-rich layers. Another sample of migmatitic gneiss from this drillhole (GSWA 182475, Kirkland et al., 2012b) yielded a maximum depositional age of 1685 ± 11 Ma (1σ). The gneissic rocks are intruded by veins of pink, coarse-grained, granite pegmatite that crystallized at 1167 ± 2 Ma (GSWA 182474, Kirkland et al., 2012a).

Two additional samples at the Big Red prospect were dated from drillhole BRDDH002, located 2.1 km to the west of BRDDH001. A sample of migmatitic gneiss (GSWA 182476, Kirkland et al., 2012c) yielded a crystallization age of 1326 ± 6 Ma for the granite protolith. Garnet-bearing mafic granulite, of which GSWA 182477 (Kirkland et al., 2012d) is representative, provided a date of 1188 ± 4 Ma, interpreted as the age of metamorphism.

Petrographic description

The sample is of migmatitic gneiss, which is fine to medium grained, grey, and contains pegmatitic leucosomes in veins and patches. The sample is composed of 40% quartz, 30% feldspar, 20% biotite, 5% garnet, 4% opaque oxide minerals, and accessory zircon, muscovite, sericite, and saussurite and epidote. Plagioclase is subhedral, clear to mildly sericitized, and albite-twinned (andesine, An39–44). Quartz is weakly elongated in polycrystalline aggregates; biotite is well aligned, and forms subhedral to euhedral flakes. Minor constituents include disseminated microcrystalline grains of opaque oxide minerals, epidote, and zircon; opaque oxide minerals are mainly associated with biotite. Garnet porphyroblasts form anhedral grains elongated parallel to the overall gneissosity of the rock. The gneiss is injected by microcrystalline aggregates and veins of sericite and saussurite (mostly clinozoisite), representing hydrothermal alteration products. Pegmatite patches and veins consist of coarse-grained mosaics of quartz, accompanied by pale-green muscovite, minor biotite, chlorite, and composite biotite–chlorite flakes.

Zircon morphology

Zircons isolated from this sample are subhedral, generally rounded, and colourless and clear to black and opaque. The crystals are up to 450 µm long, and equant to slightly elongate, with aspect ratios up to 3:1. In cathodoluminescence (CL) images, the zircons exhibit a wide range of internal structures, including idiomorphic zoning, contorted zoning, and curvilinear zoned structures. Most crystals appear to consist of older cores overgrown by at least one generation of zircon rims. A CL image of representative zircons is shown in Figure 1.

Analytical details

This sample was analysed on 22 July 2011, using
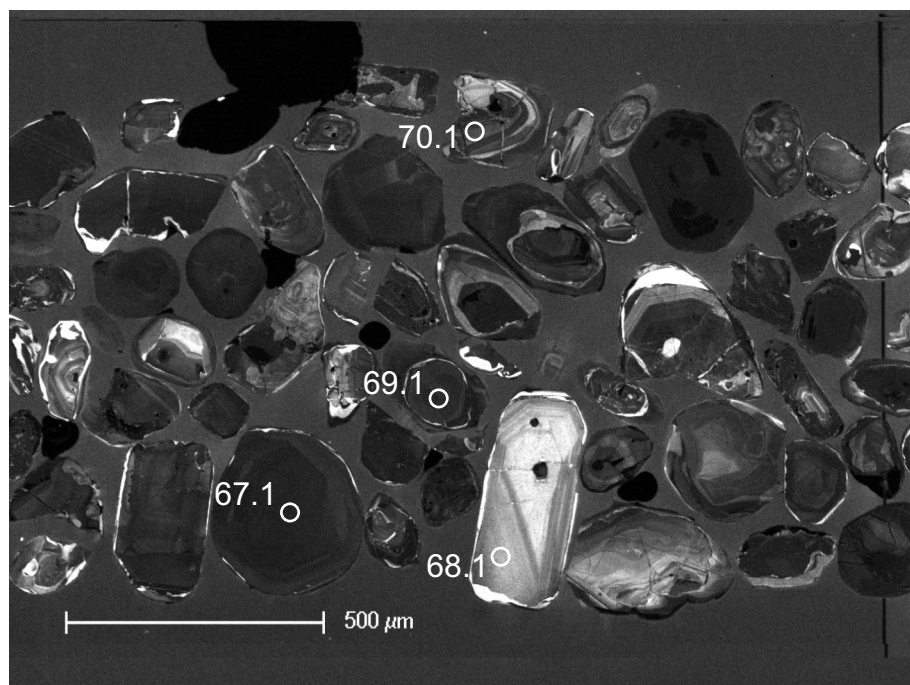
Figure 1.   **Cathodoluminescence image of representative zircons from sample 182473: migmatitic gneiss, Big Red prospect. Numbered circles indicate the approximate positions of analysis sites.**
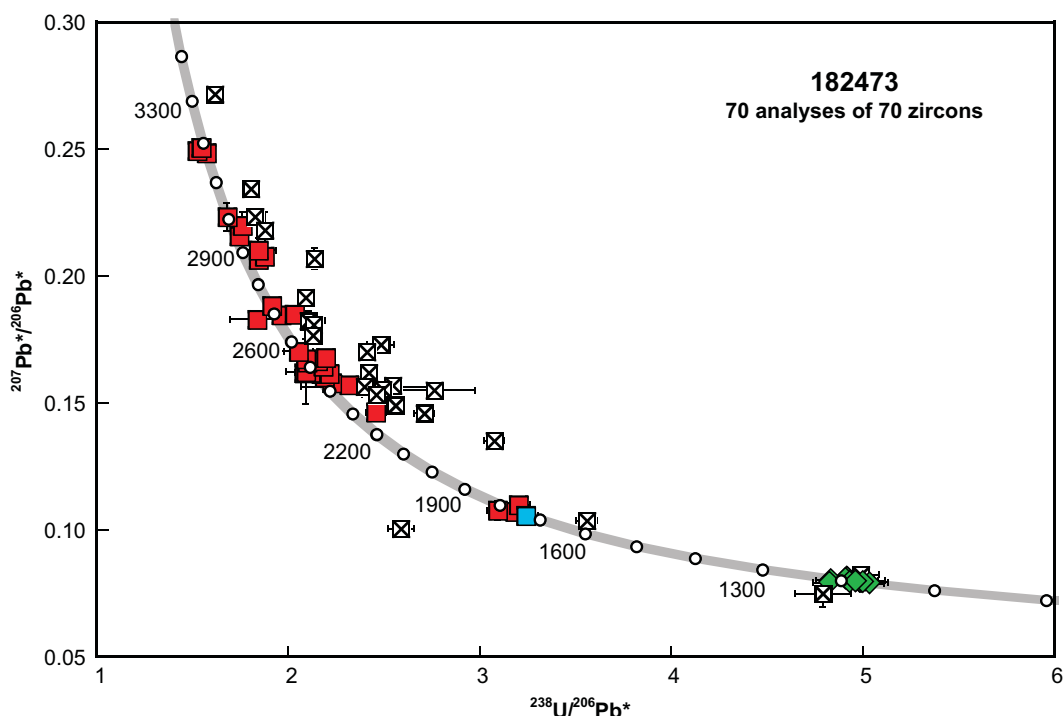
Figure 2.   **U–Pb analytical data for sample 182473: migmatitic gneiss, Big Red prospect. Blue square indicates Group Y (youngest detrital zircon); red squares indicate Group S (older detrital zircons); green diamonds indicate Group M (metamorphic zircon rims); crossed squares indicate Group D (discordance >5%).**

Table 1. Ion microprobe analytical results for zircons from sample 182473: migmatitic gneiss, Big Red prospect

| Group ID	Spot no.	Grain. spot	238U (ppm)	232Th (ppm)	232Th/238U	f204 (%)	238U/206Pb	±1σ	207Pb/206Pb	±1σ	238U/206Pb*	±1σ	207Pb*/206Pb*	±1σ	238U/206Pb* date (Ma)	±1σ	207Pb*/206Pb* date (Ma)	±1σ	Disc. (%)
Y	34	34.1	57	76	1.37	0.305	3.231	0.062	0.10848	0.00118	3.241	0.062	0.10583	0.00156	1734	30	1729	27	-0.3
S	51	51.1	110	201	1.90	0.166	3.178	0.055	0.10876	0.00095	3.183	0.055	0.10731	0.00112	1761	27	1754	19	-0.4
S	53	53.1	100	82	0.84	0.124	3.089	0.054	0.10880	0.00380	3.093	0.054	0.10772	0.00383	1806	28	1761	65	-2.5
S	37	37.1	51	38	0.76	0.089	3.198	0.063	0.11060	0.00120	3.201	0.063	0.10982	0.00132	1752	31	1796	22	2.5
S	55	55.1	48	43	0.93	0.078	2.454	0.053	0.14717	0.00173	2.456	0.053	0.14647	0.00180	2202	41	2305	21	4.5
S	50	50.1	255	238	0.96	0.028	2.317	0.035	0.15743	0.00065	2.318	0.035	0.15718	0.00066	2312	30	2426	7	4.7
S	54	54.1	172	186	1.11	0.054	2.225	0.035	0.15842	0.00355	2.226	0.035	0.15794	0.00356	2392	32	2434	38	1.7
S	12	12.1	157	96	0.63	0.017	2.187	0.031	0.16049	0.00071	2.188	0.031	0.16034	0.00072	2427	29	2459	8	1.3
S	40	40.1	174	143	0.85	0.000	2.171	0.033	0.16157	0.00080	2.171	0.033	0.16157	0.00080	2443	31	2472	8	1.2
S	42	42.1	212	86	0.42	-0.009	2.214	0.034	0.16158	0.00091	2.213	0.034	0.16166	0.00092	2403	32	2473	10	2.8
S	35	35.1	38	27	0.74	-0.072	2.082	0.044	0.16135	0.00145	2.080	0.044	0.16200	0.00152	2531	45	2477	16	-2.2
S	38	38.1	51	57	1.16	0.073	2.113	0.047	0.16290	0.00123	2.115	0.047	0.16225	0.00129	2496	47	2479	13	-0.7
S	2	2.1	155	189	1.26	0.102	2.088	0.104	0.16331	0.01285	2.090	0.104	0.16240	0.01286	2520	108	2481	134	-1.6
S	62	62.1	148	140	0.98	-0.023	2.181	0.036	0.16443	0.00085	2.180	0.036	0.16464	0.00086	2434	34	2504	9	2.8
S	7	7.1	154	112	0.75	0.143	2.096	0.029	0.16740	0.00311	2.099	0.029	0.16612	0.00313	2512	29	2519	32	0.3
S	23	23.1	104	50	0.50	0.065	2.153	0.043	0.16728	0.00100	2.154	0.043	0.16671	0.00104	2458	42	2525	11	2.6
S	39	39.1	194	104	0.55	0.013	2.092	0.031	0.16750	0.00313	2.092	0.031	0.16738	0.00313	2518	32	2532	31	0.5
S	58	58.1	219	468	2.20	0.105	2.193	0.034	0.16887	0.00075	2.196	0.034	0.16793	0.00080	2420	32	2537	8	4.6
S	67	67.1	381	79	0.21	0.021	2.053	0.076	0.17058	0.00068	2.053	0.076	0.17039	0.00069	2558	81	2561	7	0.1
S	61	61.1	102	82	0.83	-0.082	1.839	0.145	0.18214	0.00125	1.837	0.145	0.18287	0.00129	2801	192	2679	12	-4.6
S	69	69.1	314	122	0.40	0.000	1.962	0.029	0.18482	0.00061	1.962	0.029	0.18482	0.00061	2655	33	2697	5	1.5
S	25	25.1	652	263	0.42	0.009	2.033	0.036	0.18503	0.00301	2.033	0.036	0.18495	0.00301	2579	38	2698	27	4.4
S	63	63.1	137	91	0.69	0.051	1.911	0.032	0.18874	0.00091	1.912	0.032	0.18829	0.00093	2711	37	2727	8	0.6
S	36	36.1	56	44	0.81	0.038	1.843	0.035	0.20677	0.00129	1.844	0.035	0.20643	0.00131	2793	44	2878	10	2.9
S	30	30.1	180	110	0.63	-0.033	1.877	0.029	0.20759	0.00078	1.876	0.029	0.20789	0.00079	2754	35	2889	6	4.7
S	17	17.1	102	47	0.47	0.016	1.842	0.094	0.21032	0.00479	1.843	0.094	0.21018	0.00479	2795	121	2907	37	3.9
S	9	9.1	419	156	0.39	0.000	1.742	0.021	0.21565	0.00325	1.742	0.021	0.21565	0.00325	2925	29	2949	24	0.8
S	70	70.1	127	47	0.38	0.000	1.760	0.030	0.21994	0.00535	1.760	0.030	0.21994	0.00535	2901	40	2980	39	2.7
S	4	4.1	125	41	0.34	0.029	1.678	0.024	0.22355	0.00537	1.679	0.024	0.22329	0.00537	3012	35	3005	39	-0.3
S	27	27.1	179	156	0.90	0.011	1.573	0.024	0.24862	0.00082	1.573	0.024	0.24852	0.00082	3172	39	3175	5	0.1
S	13	13.1	31	33	1.08	0.080	1.522	0.034	0.25012	0.00180	1.524	0.034	0.24942	0.00184	3253	59	3181	12	-2.3
S	41	41.1	41	20	0.50	0.021	1.543	0.032	0.25079	0.00162	1.543	0.032	0.25061	0.00163	3221	54	3189	10	-1.0
M	8	8.1	128	28	0.22	0.084	5.036	0.073	0.07970	0.00091	5.041	0.073	0.07900	0.00099	1167	16	1172	25	0.5
M	24	24.1	227	1	0.01	0.000	4.831	0.088	0.07913	0.00061	4.831	0.088	0.07913	0.00061	1213	21	1176	15	-3.2
M	1	1.1	544	86	0.16	0.013	5.004	0.128	0.07961	0.00037	5.004	0.128	0.07950	0.00038	1174	28	1185	9	0.9
M	14	14.1	591	30	0.05	0.018	4.933	0.058	0.07965	0.00035	4.934	0.058	0.07950	0.00036	1190	13	1185	9	-0.4
M	18	18.1	271	51	0.20	0.000	4.989	0.091	0.07976	0.00061	4.989	0.091	0.07976	0.00061	1178	20	1191	15	1.1

Table 1. continued

| Group ID	Spot no.	Grain. spot	^{238}U (ppm)	^{232}Th (ppm)	$\dfrac{^{232}Th}{^{238}U}$	f204 (%)	$^{238}U/^{206}Pb$	± 1σ	$^{207}Pb/^{206}Pb$	± 1σ	$^{238}U/^{206}Pb*$	± 1σ	$^{207}Pb*/^{206}Pb*$	± 1σ	$^{238}U/^{206}Pb*$ date (Ma)	±1σ	$^{207}Pb*/^{206}Pb*$ date (Ma)	±1σ	Disc. (%)
M	60	60.1	734	130	0.18	0.039	4.963	0.069	0.08011	0.00037	4.965	0.069	0.07978	0.00040	1183	15	1192	10	0.7
M	16	16.1	150	47	0.33	0.038	5.016	0.097	0.08022	0.00089	5.018	0.097	0.07990	0.00095	1171	21	1194	23	1.9
M	57	57.1	1034	17	0.02	0.013	4.971	0.068	0.08002	0.00030	4.972	0.068	0.07991	0.00031	1181	15	1195	8	1.1
M	22	22.1	1326	154	0.12	0.020	4.837	0.084	0.08026	0.00027	4.838	0.084	0.08009	0.00028	1211	20	1199	7	-1.0
M	3	3.1	349	62	0.18	-0.011	5.019	0.062	0.08004	0.00047	5.018	0.062	0.08013	0.00048	1171	13	1200	12	2.4
M	6	6.1	162	34	0.22	0.022	4.986	0.069	0.08081	0.00068	4.987	0.069	0.08062	0.00070	1178	15	1212	17	2.8
M	11	11.1	238	122	0.53	0.015	4.915	0.063	0.08080	0.00056	4.916	0.063	0.08067	0.00057	1194	14	1214	14	1.6
M	52	52.1	449	63	0.14	-0.056	4.929	0.070	0.08066	0.00049	4.926	0.070	0.08113	0.00053	1191	16	1225	13	2.7
M	44	44.1	222	40	0.18	-0.043	4.924	0.076	0.08093	0.00068	4.922	0.076	0.08129	0.00073	1192	17	1229	18	3.0
D	45	45.1	20	0	0.01	1.226	4.734	0.143	0.08527	0.00239	4.793	0.147	0.07498	0.00525	1222	35	1068	141	-14.4
D	33	33.1	61	1	0.01	0.057	4.989	0.093	0.08282	0.00110	4.992	0.093	0.08234	0.00121	1177	20	1254	29	6.1
D	19	19.1	29	23	0.80	0.150	2.585	0.068	0.10179	0.00164	2.589	0.068	0.10049	0.00189	2105	48	1633	35	-28.9
D	49	49.1	214	135	0.65	0.044	3.556	0.055	0.10393	0.00067	3.558	0.055	0.10355	0.00071	1597	22	1689	13	5.4
D	5	5.1	64	31	0.50	0.146	3.071	0.053	0.13640	0.00114	3.076	0.053	0.13510	0.00128	1815	28	2165	17	16.2
D	28	28.1	63	80	1.31	0.033	2.708	0.052	0.14629	0.00130	2.709	0.052	0.14600	0.00133	2025	34	2300	16	11.9
D	43	43.1	109	86	0.82	0.019	2.559	0.044	0.14930	0.00100	2.560	0.044	0.14914	0.00101	2126	32	2336	12	9.0
D	26	26.1	348	100	0.30	0.000	2.458	0.075	0.15340	0.00254	2.458	0.075	0.15340	0.00254	2200	59	2384	28	7.7
D	46	46.1	336	105	0.32	0.223	2.756	0.214	0.15719	0.00067	2.762	0.214	0.15520	0.00076	1992	142	2404	8	17.1
D	47	47.1	270	99	0.38	-0.029	2.496	0.037	0.15523	0.00065	2.495	0.037	0.15549	0.00066	2173	28	2407	7	9.7
D	68	68.1	32	24	0.78	0.186	2.394	0.332	0.15815	0.00190	2.399	0.332	0.15649	0.00213	2246	298	2418	23	7.1
D	20	20.1	312	138	0.46	0.049	2.544	0.046	0.15743	0.00073	2.545	0.046	0.15700	0.00075	2136	33	2424	8	11.9
D	29	29.1	179	21	0.12	0.028	2.422	0.037	0.16225	0.00313	2.423	0.037	0.16200	0.00314	2227	29	2477	33	10.1
D	10	10.1	106	144	1.40	0.000	2.411	0.036	0.17015	0.00113	2.411	0.036	0.17015	0.00113	2237	29	2559	11	12.6
D	31	31.1	647	48	0.08	-0.005	2.483	0.070	0.17300	0.00153	2.483	0.070	0.17304	0.00154	2182	53	2587	15	15.7
D	65	65.1	536	343	0.66	0.034	2.127	0.030	0.17686	0.00047	2.128	0.030	0.17656	0.00048	2483	29	2621	5	5.2
D	64	64.1	86	70	0.84	0.042	2.130	0.039	0.18111	0.00125	2.131	0.039	0.18074	0.00128	2480	38	2660	12	6.7
D	21	21.1	191	78	0.42	-0.026	2.107	0.086	0.18214	0.00401	2.106	0.086	0.18237	0.00401	2504	87	2675	36	6.4
D	56	56.1	160	113	0.73	-0.010	2.092	0.034	0.19163	0.00088	2.092	0.034	0.19171	0.00088	2518	34	2757	8	8.7
D	66	66.1	216	110	0.52	0.109	2.132	0.033	0.20786	0.00427	2.135	0.033	0.20689	0.00428	2477	32	2881	34	14.0
D	15	15.1	133	53	0.41	0.008	1.876	0.027	0.21819	0.00708	1.877	0.027	0.21812	0.00708	2754	33	2967	52	7.2
D	32	32.1	310	312	1.04	-0.014	1.827	0.026	0.22325	0.00060	1.827	0.026	0.22338	0.00060	2815	33	3005	4	6.3
D	48	48.1	134	26	0.20	0.010	1.803	0.031	0.23441	0.00130	1.803	0.031	0.23431	0.00131	2845	40	3082	9	7.7
D	59	59.1	125	76	0.62	-0.008	1.616	0.027	0.27168	0.00106	1.616	0.027	0.27175	0.00106	3106	42	3316	6	6.3
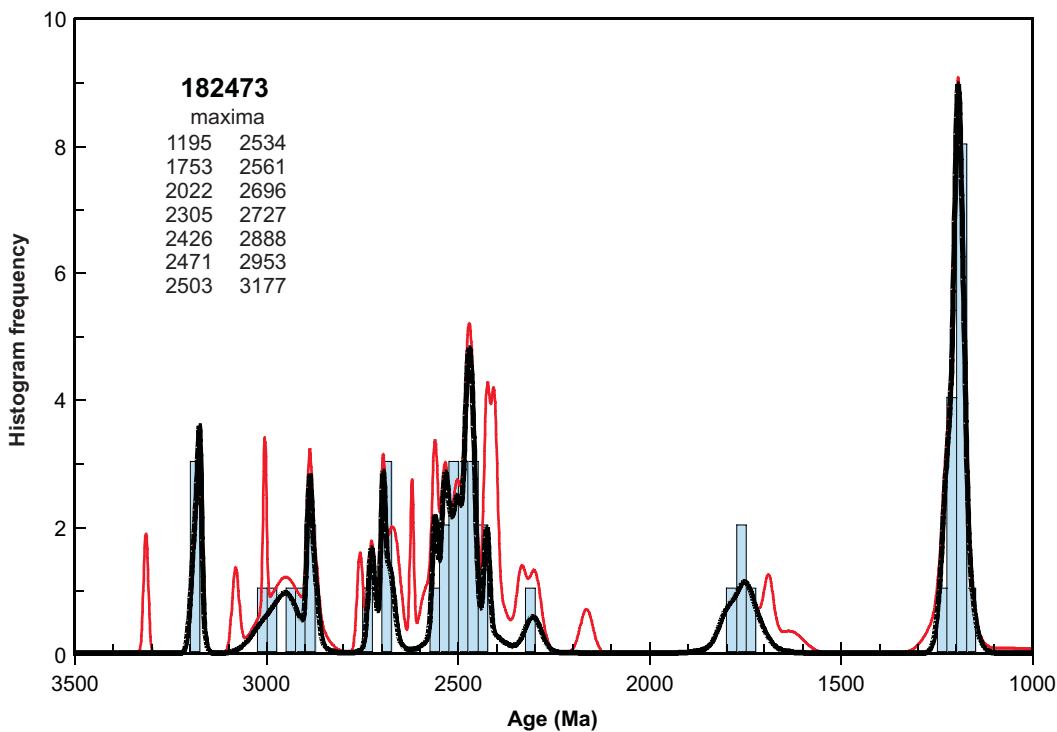
Figure 3. Probability density diagram and histogram for sample 182473: migmatitic gneiss, Big Red prospect. Thick curve, maxima values, and frequency histogram (bin width 25 Ma) only include data with discordance <5% (46 analyses of 46 zircons). Thin curve includes all data (70 analyses of 70 zircons).

SHRIMP-B, on 28 July 2011, using SHRIMP-A, and on 20–21 October 2011, using SHRIMP-B. Analyses 1.1 to 15.1 (spot numbers 1–15) were obtained during the first session, together with nine analyses of the BR266 standard, of which seven analyses indicated an external spot-to-spot (reproducibility) uncertainty of 0.99% (1σ) and a ^{238}U/^{206}Pb* calibration uncertainty of 0.39% (1σ). Analyses 16.1 to 25.1 (spot numbers 16–25) were obtained during the second session, together with eight analyses of the BR266 standard, of which seven analyses indicated an external spot-to-spot (reproducibility) uncertainty of 1.60% (1σ) and a ^{238}U/^{206}Pb* calibration uncertainty of 0.60% (1σ). Analyses 26.1 to 70.1 (spot numbers 26–70) were obtained during the third session, together with 21 analyses of the BR266 standard, of which 17 analyses indicated an external spot-to-spot (reproducibility) uncertainty of 1.25% (1σ) and a ^{238}U/^{206}Pb* calibration uncertainty of 0.32% (1σ). Calibration uncertainties are included in the errors of ^{238}U/^{206}Pb* ratios and dates listed in Table 1. Common-Pb corrections were applied to all analyses using contemporaneous isotopic compositions determined according to the model of Stacey and Kramers (1975).

Results

Seventy analyses were obtained from 70 zircons. Results are listed in Table 1, and shown in a concordia diagram (Fig. 2) and a probability density diagram (Fig. 3).

Interpretation

The analyses are concordant to discordant (Fig. 2). Twenty-four analyses are >5% discordant (Group D). The dates obtained from these 24 analyses (Group D; Table 1) are imprecise or unreliable, and are considered not to be geologically significant. The remaining 46 analyses can be divided into three groups, based on their ^{207}Pb*/^{206}Pb* ratios and locations within the crystals.

Group Y comprises one analysis of a zircon core (Table 1), which yields a ^{207}Pb*/^{206}Pb* date of 1729 ± 27 Ma (1σ).

Group S comprises 31 analyses of zircon cores (Table 1), which yield ^{207}Pb*/^{206}Pb* dates of 3189–1754 Ma.

Group M comprises 14 analyses of zircon rims (Table 1), which yield a concordia age of 1193 ± 5 Ma (MSWD = 1.1).

It is possible that all of the analyses in Groups Y and S are of unmodified detrital zircons, in which case the date of 1729 ± 27 Ma (1σ) for the single analysis in Group Y represents a maximum depositional age for the sedimentary precursor of the gneiss. A more conservative estimate of the maximum depositional age is provided by the weighted mean ^{207}Pb*/^{206}Pb* date of 1763 ± 47 Ma (MSWD = 1.4) for the four youngest analyses in combined Groups Y and S.

The 32 analyses in combined Groups Y and S indicate dates that define significant age components at c. 3177,

2696, 2575–2450, and 1753 Ma, and several minor components between 3189 and 1754 Ma. These are interpreted as the ages of zircon-crystallizing rocks in the detrital source region(s), or as the ages of detrital components within sediments that have been reworked into this rock. These age components are consistent with this paragneiss belonging to either the Paleoproterozoic Barren Basin or to the Mesoproterozoic Arid Basin (Spaggiari et al., 2011).

The date of 1193 ± 5 Ma for the 14 zircon rim analyses in Group M is interpreted as the age of a high-grade metamorphic and migmatization event during Stage II of the Albany–Fraser Orogeny (1215–1140 Ma; Clark et al., 2000).

References

Clark, DJ, Hensen, BJ and Kinny, PD 2000, Geochronological constraints for a two-stage history of the Albany–Fraser Orogen, Western Australia: Precambrian Research, v. 102, no. 3, p. 155–183.

Kirkland, CL, Wingate, MTD and Spaggiari, CV 2012a, 182474: granite vein, Big Red prospect; Geochronology Record 1051: Geological Survey of Western Australia, 4p.

Kirkland, CL, Wingate, MTD and Spaggiari, CV 2012b, 182475: migmatitic gneiss, Big Red prospect; Geochronology Record 1052: Geological Survey of Western Australia, 7p.

Kirkland, CL, Wingate, MTD and Spaggiari, CV 2012c, 182476: migmatitic gneiss, Big Red prospect; Geochronology Record 1053: Geological Survey of Western Australia, 4p.

Kirkland, CL, Wingate, MTD and Spaggiari, CV 2012d, 182477: mafic granulite, Big Red prospect; Geochronology Record 1055: Geological Survey of Western Australia, 4p.

Nelson, DR, Myers, JS and Nutman, AP 1995, Chronology and evolution of the Middle Proterozoic Albany–Fraser Orogen, Western Australia: Australian Journal of Earth Sciences, v. 42, p. 481–495, DOI:10.1080/08120099508728218.

Spaggiari, CV, Kirkland, CL, Pawley, MJ, Smithies, RH, Wingate, MTD, Doyle, MG, Blenkinsop, TG, Clark, C, Oorschot, CW, Fox, LJ and Savage, J 2011, The geology of the east Albany–Fraser Orogen — a field guide: Geological Survey of Western Australia, Record 2011/23, 98p.

Stacey, JS and Kramers, JD 1975, Approximation of terrestrial lead isotope evolution by a two-stage model: Earth and Planetary Science Letters, v. 26, p. 207–221.

Tillick, D 2010, Final report of co-funded government–industry drilling program at the Eucla Project, E28/1608, September 2010; Teck Australia Pty Ltd: Geological Survey of Western Australia, Statutory mineral exploration report, A88011, 23p. (unpublished).

Recommended reference for this publication